Hydrogen Isotopic Composition of Hydrous Minerals in Asteroid Ryugu

Laurette Piani, Kazuhide Nagashima, Noriyuki Kawasaki, Naoya Sakamoto, Ken-Ichi Bajo, Yoshinari Abe, Jérôme Aléon, Conel M. O'D. Alexander, Sachiko Amari, Yuri Amelin, et al.

The Astrophysical Journal Letters, 946:L43 (11pp), 2023 April 1 https://doi.org/10.3847/2041-8213/acc393

Hydrogen Isotopic Composition of Hydrous Minerals in Asteroid Ryugu

Laurette Piani[1], Kazuhide Nagashima[2], Noriyuki Kawasaki[3], Naoya Sakamoto[4], Ken-ichi Bajo[3], Yoshinari Abe[5], Jérôme Aléon[6], Conel M. O'D. Alexander[7], Sachiko Amari[8,9], Yuri Amelin[10], Martin Bizzarro[11], Audrey Bouvier[12], Richard W. Carlson[7], Marc Chaussidon[13], Byeon-Gak Choi[14], Nicolas Dauphas[15], Andrew M. Davis[15], Tommaso Di Rocco[16], Wataru Fujiya[17], Ryota Fukai[18], Ikshu Gautam[19], Makiko K. Haba[19], Yuki Hibiya[20], Hiroshi Hidaka[21], Hisashi Homma[22], Peter Hoppe[23], Gary R. Huss[2], Kiyohiro Ichida[24], Tsuyoshi Iizuka[25], Trevor R. Ireland[26], Akira Ishikawa[19], Shoichi Itoh[27], Noriko T. Kita[28], Kouki Kitajima[28], Thorsten Kleine[29], Shintaro Komatani[24], Alexander N. Krot[2], Ming-Chang Liu[30], Yuki Masuda[19], Kevin D. McKeegan[30], Mayu Morita[24], Kazuko Motomura[31], Frédéric Moynier[13], Izumi Nakai[32], Ann Nguyen[33], Larry Nittler[7], Morihiko Onose[24], Andreas Pack[16], Changkun Park[34], Liping Qin[35], Sara S. Russell[36], Maria Schönbächler[37], Lauren Tafla[30], Haolan Tang[30], Kentaro Terada[38], Yasuko Terada[39], Tomohiro Usui[17], Sohei Wada[3], Meenakshi Wadhwa[40], Richard J. Walker[41], Katsuyuki Yamashita[42], Qing-Zhu Yin[43], Tetsuya Yokoyama[19], Shigekazu Yoneda[44], Edward D. Young[30], Hiroharu Yui[45], Ai-Cheng Zhang[46], Tomoki Nakamura[47], Hiroshi Naraoka[48], Ryuji Okazaki[48], Kanako Sakamoto[18], Hikaru Yabuta[49], Masanao Abe[18], Akiko Miyazaki[18], Aiko Nakato[18], Masahiro Nishimura[18], Tatsuaki Okada[18], Toru Yada[18], Kasumi Yogata[18], Satoru Nakazawa[18], Takanao Saiki[18], Satoshi Tanaka[18], Fuyuto Terui[50], Yuichi Tsuda[18], Sei-ichiro Watanabe[21], Makoto Yoshikawa[18], Shogo Tachibana[51], and Hisayoshi Yurimoto[3,4]

[1] Centre de Recherches Pétrographiques et Géochimiques, CNRS—Université de Lorraine; F-54500 Nancy, France; laurette.piani@univ-lorraine.fr
[2] Hawai'i Institute of Geophysics and Planetology, University of Hawai'i at Mānoa; Honolulu, HI 96822, USA
[3] Department of Natural History Sciences, Hokkaido University, Sapporo 060-0810, Japan
[4] Isotope Imaging Laboratory, Creative Research Institution, Hokkaido University, Sapporo 001-0021, Japan
[5] Graduate School of Engineering Materials Science and Engineering, Tokyo Denki University, Tokyo 120-8551, Japan
[6] Institut de Minéralogie, de Physique des Matériaux et de Cosmochimie, Sorbonne Université, Museum National d'Histoire Naturelle, CNRS UMR 7590, IRD; F-75005 Paris, France
[7] Earth and Planets Laboratory, Carnegie Institution for Science, Washington, DC, 20015, USA
[8] McDonnell Center for the Space Sciences and Physics Department, Washington University, St. Louis, MO 63130, USA
[9] Geochemical Research Center, The University of Tokyo, Tokyo, 113-0033, Japan
[10] Guangzhou Institute of Geochemistry, Chinese Academy of Sciences, Guangzhou, GD 510640, People's Republic of China
[11] Centre for Star and Planet Formation, GLOBE Institute, University of Copenhagen, Copenhagen, DK-1350, Denmark
[12] Bayerisches Geoinstitut, Universität Bayreuth, Bayreuth D-95447, Germany
[13] Université Paris Cité, Institut de physique du globe de Paris, CNRS, F-75005 Paris, France
[14] Department of Earth Science Education, Seoul National University, Seoul 08826, Republic of Korea
[15] Department of the Geophysical Sciences and Enrico Fermi Institute, The University of Chicago, Chicago, IL 60637, USA
[16] Faculty of Geosciences and Geography, University of Göttingen, Göttingen, D-37077, Germany
[17] Faculty of Science, Ibaraki University, Mito 310-8512, Japan
[18] ISAS/JSEC, JAXA, Sagamihara 252-5210, Japan
[19] Department of Earth and Planetary Sciences, Tokyo Institute of Technology, Tokyo 152-8551, Japan
[20] General Systems Studies, The University of Tokyo, Tokyo 153-0041, Japan
[21] Earth and Planetary Sciences, Nagoya University, Nagoya 464-8601, Japan
[22] Osaka Application Laboratory, SBUWDX, Rigaku Corporation, Osaka 569-1146, Japan
[23] Max Planck Institute for Chemistry, Mainz D-55128, Germany
[24] Analytical Technology, Horiba Techno Service Co., Ltd., Kyoto 601-8125, Japan
[25] Earth and Planetary Science, The University of Tokyo, Tokyo 113-0033, Japan
[26] School of Earth and Environmental Sciences, The University of Queensland, St Lucia QLD 4072, Australia
[27] Division of Earth and Planetary Sciences, Kyoto University, Kitashirakawaoiwake-cho, Sakyo-ku, Kyoto 606-8502, Japan
[28] Geoscience, University of Wisconsin-Madison Madison, WI 53706, USA
[29] Max Planck Institute for Solar System Research, D-37077 Göttingen, Germany
[30] Earth, Planetary, and Space Sciences, UCLA, Los Angeles, CA 90095, USA
[31] Thermal Analysis, Rigaku Corporation, Tokyo 196-8666, Japan
[32] Applied Chemistry, Tokyo University of Science, Tokyo 162-8601, Japan
[33] Astromaterials Research and Exploration Science, NASA Johnson Space Center, Houston, TX 77058, USA
[34] Earth-System Sciences, Korea Polar Research Institute, Incheon 21990, Republic of Korea
[35] University of Science and Technology of China, School of Earth and Space Sciences, Anhui 230026, People's Republic of China
[36] Department of Earth Sciences, Natural History Museum, London, SW7 5BD, UK
[37] Institute for Geochemistry and Petrology, Department of Earth Sciences, ETH Zurich, Zurich, Switzerland
[38] Earth and Space Science, Osaka University, Osaka 560-0043, Japan
[39] Spectroscopy and Imaging, Japan Synchrotron Radiation Research Institute, Hyogo 679-5198 Japan
[40] School of Earth and Space Exploration, Arizona State University, Tempe, AZ 85281, USA
[41] Department of Geology, University of Maryland, College Park, MD 20742, USA
[42] Graduate School of Natural Science and Technology, Okayama University, Okayama 700-8530, Japan
[43] Earth and Planetary Sciences, University of California, Davis, CA 95616, USA
[44] Science and Engineering, National Museum of Nature and Science; Tsukuba 305-0005, Japan
[45] Chemistry, Tokyo University of Science, Tokyo 162-8601, Japan
[46] School of Earth Sciences and Engineering, Nanjing University, Nanjing 210023, People's Republic of China
[47] Department of Earth Science, Tohoku University, Sendai, 980-8578, Japan
[48] Department of Earth and Planetary Sciences, Kyushu University, Fukuoka 819-0395, Japan
[49] Earth and Planetary Systems Science Program, Hiroshima University, Higashi-Hiroshima, 739-8526, Japan

[50] Kanagawa Institute of Technology, Atsugi 243-0292, Japan
[51] UTokyo Organization for Planetary and Space Science, University of Tokyo, Tokyo 113-0033, Japan
Received 2022 December 20; revised 2023 February 23; accepted 2023 March 6; published 2023 April 4

Abstract

Rock fragments of the Cb-type asteroid Ryugu returned to Earth by the JAXA Hayabusa2 mission share mineralogical, chemical, and isotopic properties with the Ivuna-type (CI) carbonaceous chondrites. Similar to CI chondrites, these fragments underwent extensive aqueous alteration and consist predominantly of hydrous minerals likely formed in the presence of liquid water on the Ryugu parent asteroid. Here we present an in situ analytical survey performed by secondary ion mass spectrometry from which we have estimated the D/H ratio of Ryugu's hydrous minerals, D/H_{Ryugu}, to be $[165 \pm 19] \times 10^{-6}$, which corresponds to $\delta D_{Ryugu} = +59 \pm 121‰$ (2σ). The hydrous mineral D/H_{Ryugu}'s values for the two sampling sites on Ryugu are similar; they are also similar to the estimated D/H ratio of hydrous minerals in the CI chondrites Orgueil and Alais. This result reinforces a link between Ryugu and CI chondrites and an inference that Ryugu's samples, which avoided terrestrial contamination, are our best proxy to estimate the composition of water at the origin of hydrous minerals in CI-like material. Based on this data and recent literature studies, the contribution of CI chondrites to the hydrogen of Earth's surficial reservoirs is evaluated to be ~3%. We conclude that the water responsible for the alteration of Ryugu's rocks was derived from water ice precursors inherited from the interstellar medium; the ice partially re-equilibrated its hydrogen with the nebular H_2 before being accreted on the Ryugu's parent asteroid.

Unified Astronomy Thesaurus concepts: Carbonaceous chondrites (200); Earth (planet) (439); Asteroids (72); Ice composition (2272); Solar system (1528); Small Solar System bodies (1469); Planetary science (1255); Chondrites (228); Meteorites (1038); Meteorite composition (1037)

1. Introduction

The first analyses of samples of asteroid Ryugu brought back by the JAXA Hayabusa2 mission revealed their similarity to CI (Ivuna-type) carbonaceous chondrites (Yokoyama et al. Yokoyama et al. 2023). Like CIs, Ryugu's samples underwent extensive aqueous alteration on their parent asteroid in the presence of liquid water and consist predominantly of hydrous silicates (serpentine, saponite) and other secondary minerals (i.e., carbonates, magnetites, sulfides) that likely formed during asteroidal fluid circulation (Ito et al. 2022; Nakamura et al. 2022a, 2022b; Moynier et al. 2022; Yokoyama et al. 2023). However, the Ryugu samples are depleted in hydrogen and oxygen compared to CI chondrites, as indicated by the difference in the abundance of water in Ryugu and Ivuna: 6.84 versus 12.73 wt.% H_2O equivalent, respectively (Yokoyama et al. 2023) and by the difference in oxygen abundance measured by X-ray fluorescence spectroscopy (Yokoyama et al. 2023; Nakamura et al. 2022a). Thermogravimetric analysis coupled with mass spectrometry indicated that the water depletion is likely a consequence of the loss of interlayer water in Ryugu's saponite phyllosilicates to space after the formation of Ryugu's parent body (Yokoyama et al. 2023). The high abundance of interlayer water in CI chondrites compared to Ryugu's rocks indicates that either CI chondrites did not experience a similar water loss in space or that CI chondrites acquired their interlayer water during their residence on Earth (Yokoyama et al. 2023).

Hydrogen isotopes (^1H and ^2H, also called D for deuterium) show large variations among planetary materials and can thus help us to understand the source and distribution of water and volatile elements in the protoplanetary disk (e.g., Robert & Epstein 1982; Alexander et al. 2012; McCubbin & Barnes 2019; Vacher et al. 2020; Piani et al. 2021). The first reports for Ryugu indicated that its bulk hydrogen isotopic composition $\delta D = 252‰ \pm 13‰$, expressed in δ notation (‰) relative to the standard mean ocean water ratio $D/H_{SMOW} = 155.76 \times 10^{-6}$ (Naraoka et al. 2023), is higher than most of the values measured so far for bulk CI chondrites: Orgueil $\delta D = +182‰ \pm 44‰$, Ivuna $\delta D = +232 \pm 60‰$ and Alais $\delta D = +89‰ \pm 63‰$ (± 2 standard deviations; data compilation in Piani et al. 2021). In contrast, the D/H of the insoluble organic matter (IOM) obtained after mineral removal by acid dissolution appears be lower in Ryugu ($\delta D = +306‰$ and $+440‰$ for sites A and C, respectively; Yabuta et al. 2023) than in the IOM of CI chondrites ($\delta D \approx +1000‰$; Alexander et al. 2007).

Direct estimates of the water D/H ratios cannot be obtained easily in chondritic material due to the difficulty in estimating the organic matter contribution to the bulk hydrogen concentration and D/H ratios. Water D/H ratios in chondrites have been approximated by the bulk D/H composition or estimated by mass balance calculations to remove the contribution of the organic components (e.g., Robert & Epstein 1982; Alexander et al. 2010). In mass balance calculations, organic concentrations and D/H compositions are generally measured after solvent extraction (Yamashita & Naraoka 2014) or chemical isolation from minerals (Alexander et al. 2007). However, about half of the total organic matter might not be accessible with these techniques (Alexander et al. 2015; Viennet et al. 2022), resulting in high and poorly constrained uncertainties. Alexander et al. (2012) developed a powerful technique to estimate the water isotopic composition of chondritic parent bodies based on measurements of D/H and C/H ratios of the whole rock chondrites. The technique was applied to CM (Mighei-type) and CR (Renazzo-type) chondrites for which large numbers of meteorites are available, but this method cannot be applied to individual samples. More recently, an in situ analytical method based on the analyses of the C/H and D/H ratios of chondritic fine-grained material by secondary ion mass spectrometry (SIMS) was applied to individual carbonaceous chondrites to estimate the D/H ratio of hydrogen retained in the hydrous minerals (Piani et al.2018).

Table 1
Hydrous Mineral D/H Ratios Estimated from SIMS Measurements

Sample	Type	N	Pearson Coeff.	$(D/H)_0 \times 10^{-6}$	Error $\times 10^{-6}$	$D/H_{water} \times 10^{-6}$	Error $\times 10^{-6}$	δD (‰)	Error (‰)
Mighei	CM2	21	0.57	96	8	95	21	−388	134
Orgueil	CI	18	0.68	117	14	141	24	−98	153
Orgueil[a]	CI	17	0.70	119	11	146	22	−63	138
A0040	Ryugu site A	30	0.48	125	20	159	31	20	197
A0094	Ryugu site A	28	0.72	118	17	143	27	−79	175
C0002	Ryugu site C	37	0.49	124	26	156	36	−1	233
All Ryugu	Ryugu all	95	0.57	127	10	164	21	50	135
All Ryugu[a]	Ryugu all	90	0.72	128	6	165	19	59	121

Note. N = number of SIMS analytical spots; Pearson coeff. = Pearson correlation coefficient; $(D^-/H^-)_0$=zero intercept of the D/H vs. C/H correlation measured in the chondrite matrix or for Ryugu particles.
[a] Data with analyses outside of the main trend removed (removal of all points outside the prediction interval at 95%; see Figure A4)

Here, we report on the hydrogen isotopic composition in Ryugu's particles from the two landing sites. The estimated D/H ratio of Ryugu's hydrous minerals is compared to hydrous mineral D/H ratios measured by the same method in carbonaceous chondrites from different groups, including CI chondrites in order to discuss the possible relationship between water present on Ryugu's and other carbonaceous chondrites' parent bodies.

2. Material and Methods

D/H measurements were performed by SIMS on three separate mechanical fragments from stones A0040 and A0094 from the first touchdown site and stone C0002 from the second touchdown site, collected by the Hayabusa2 spacecraft during its two touchdowns on the asteroid Ryugu (Tachibana et al. 2022), as well as material from the CM2 chondrite Mighei and CI chondrite Orgueil also analyzed in previous studies (Piani et al. 2018, 2021; Table 1). Submillimeter Ryugu fragments were handpicked under a stereomicroscope and pressed into pure indium. In order to avoid contamination and loss of soluble organic compounds, the pressed samples were not polished or exposed to solvents. The flattest areas were then identified using a polarized reflected-light microscope, and backscattered electron (BSE) images and X-ray elemental maps were acquired by energy dispersive spectroscopy (EDS; Figures 1, A1–A2). Areas with large anhydrous silicates or holes were avoided based on EDS maps. A final verification using BSE/EDS was performed after SIMS measurements (Figures 1, A1–A2). Analyses with positions that did not correspond to flat, fine-grained matrix or contained cracks/holes were removed from the final data set (as provided on ORDaR[52]). The samples were stored under vacuum before and after analyses and were introduced in the SIMS instrument several days before measurements.

Reference materials, including hydrated minerals (two amphiboles, a montmorillonite, and a serpentine), three hydrogen-bearing glasses, a terrestrial kerogen, and two extraterrestrial D-rich organic matter samples, were used for calibration and correction for instrumental mass fractionation on the D/H ratio (Table A1; Figure A3). Polished pieces of the Kipawa amphibole were mounted on each mount containing Ryugu and Orgueil material and were systematically measured for comparison. All mounts of samples and standards were prepared with indium and gold coated before analysis.

The SIMS analyses were performed using the CAMECA IMS-1280HR2 instrument at CRPG (France). A Cs^+ primary beam accelerated at 10 kV was rastered, and the H^-, D^-, $^{13}C^-$, and $^{29}Si^-$ ion signals were collected from 12×12 μm^2 areas. The analytical conditions are similar to previous studies (Piani et al. 2018, 2021) and are detailed in the Appendix. The statistical error on D/H in the sample having the lowest D/H ratio was 3% (2σ standard deviation), and the reproducibility on the reference materials was $\leqslant$7% (2σ).

The zero intercept of the D^-/H^- versus C^-/H^- correlation in each chondrite's matrix calculated using a simple least-square fit was used to establish the D/H ratio of hydrous silicates in that chondrite (Table 1). Because the errors on analytical points are all of the same range (Figure 2), a linear regression calculated using a simple least-square fit gives similar slope and zero intercept than a linear fit taking into account the analytical uncertainties and error correlations. We thus used a simple least-square fit for simplicity. The D/H ratios estimated for hydrous minerals in chondrites, $(D/H)_0$, were corrected for instrumental mass fractionation using a calibration line (measured versus known) determined using all standard materials including hydrous minerals, glasses, the terrestrial kerogen, and the D-rich IOMs to correct simultaneously for the background contamination (Figure S3 in Remusat et al. 2016). The slope of the calibration line is 2.2 ± 0.2, and the intercept is $[-1.16 \pm 0.36] \times 10^{-4}$ with errors at 95% confidence. For estimating the error on the final D/H ratios, we propagated the 95% error on the zero intercept obtained for the samples and the corresponding 2σ error on the standard calibration.

3. Results

After removal of all analyses in which holes or cracks were observed by the post-analysis survey, we obtained 95 analyses of the D/H and C/H ratios in the three fragments of Ryugu, C0002, A0040, and A0094 (Figure 2). The ranges of D/H and C/H ratios obtained for the two landing sites are similar, but particle A0094 shows lower values than particles A0040 and C0002 for both ratios (Figure 2(A)). Most of the data obtained for Ryugu's particles define a positive correlation between the

[52] doi:10.24396/ORDAR-107

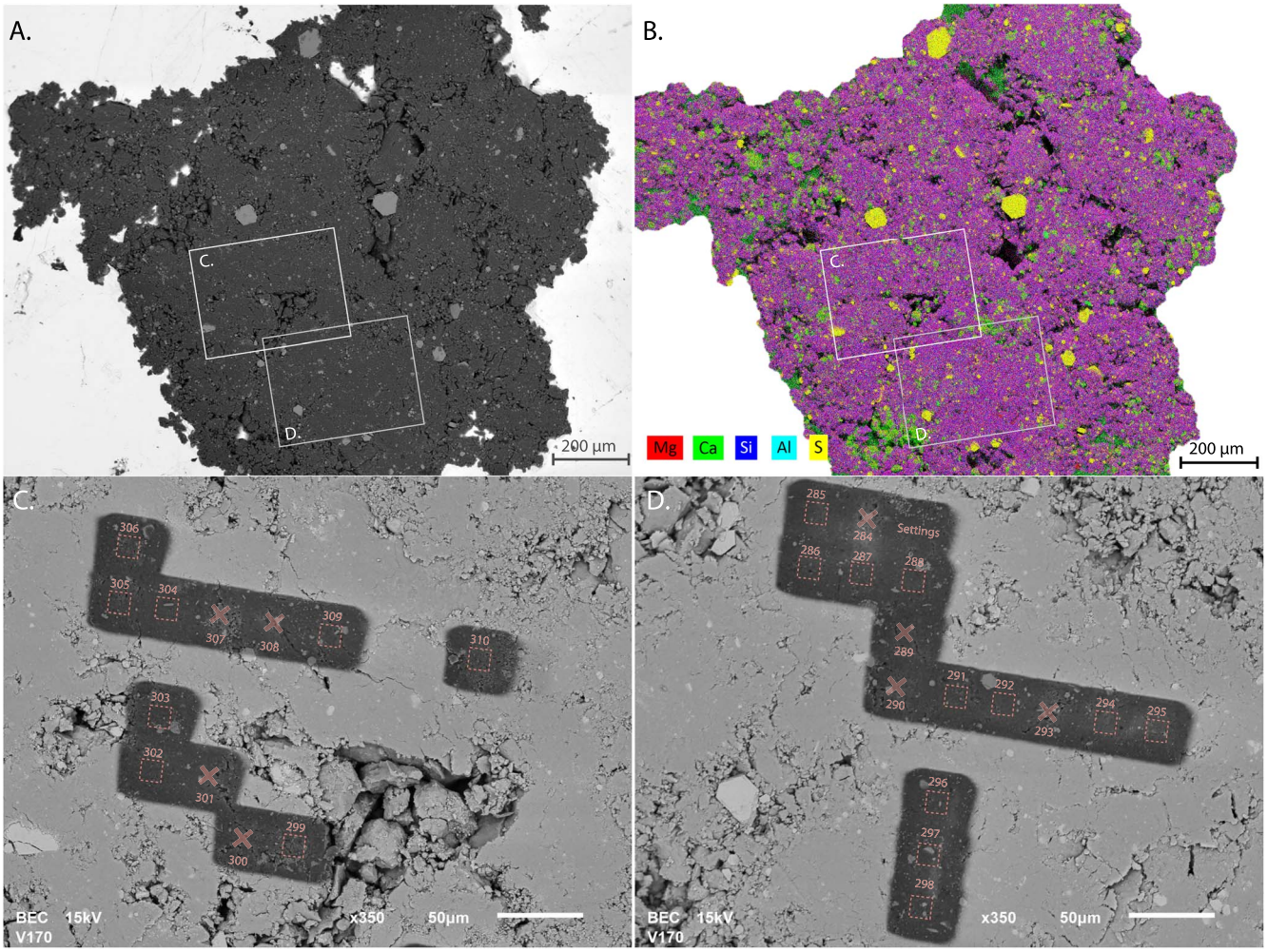

Figure 1. Scanning electron microscope (SEM) images of a piece of particle A0040 pressed in indium and location of the SIMS analyses. (A) Backscattered electron (BSE) image of the pressed particle fragment before SIMS analyses. (B) Combined X-ray elemental map of the particle fragment. The particle is dominated by Mg-rich phyllosilicates (purple), sulfides (yellow), and carbonates (light green). Large holes and cracks (black) were avoided for SIMS analyses. (C)–(D) BSE images of areas measured by SIMS. The numbers correspond to the analysis numbers as provided on ORDaR.[53] Red crosses indicate analyses that were rejected due to small holes or cracks identified by SEM after the SIMS measurements.

D/H and the C/H ratios, but five points are located significantly above the main trend, outside of the prediction interval at 95% (Figures 2(A) and A4). The correlation described by the 90 other points is defined with a Pearson correlation coefficient of 0.72 and a zero intercept of the least-square fit of $(D/H)_0 = [128 \pm 64] \times 10^{-6}$ (Table 1). Using the calibration line defined on standards (Figure A3), the estimated D/H ratio of the Ryugu's hydrous mineral, D/H_{Ryugu}, is $[165 \pm 19] \times 10^{-6}$, which corresponds to δD_{Ryugu} of $+59‰ \pm 121‰$ (2σ).

The Orgueil (CI) and Mighei (CM) chondrites measured in the same SIMS session also show positive correlations between the D/H and the C/H ratios (Figure 2) with Pearson coefficients of 0.68 and 0.57 (Table 1). For Orgueil, one point lies outside of the prediction interval at 95% (Figure A4). The correlation defined by the 17 other points has a Pearson correlation coefficient of 0.70 and a zero intercept of $(D/H)_0 = [119 \pm 11] \times 10^{-6}$ (Table 1 Mighei displays a zero intercept of $D/H_0 = [96 \pm 8] \times 10^{-6}$ (Table 1), with no outliers. Using the standard calibration line (Figure A3), we estimate that the hydrogen isotopic compositions of Orgueil and Mighei hydrous silicates are $\delta D_{Orgueil} = -63‰ \pm 138‰$ and $\delta D_{Mighei} = -388‰ \pm 134‰$ (2σ), which are consistent, within error, with previous measurements of CM (Piani et al. 2018) and CI chondrites (Piani et al. 2021).

4. Discussion

4.1. Water H-isotopic Compositions of Ryugu and CI Chondrites

The hydrous silicate D/H estimated for Ryugu of $\delta D_{Ryugu} = +59‰ \pm 121‰$ (2σ) is similar, within errors, to our D/H estimations for hydrous minerals in the CI carbonaceous chondrite Orgueil that was determined in the same session of measurement (Table 1) and for hydrous minerals in CI, chondrites, CV chondrites, and the least altered lithologies of the CM chondrite Paris in our previous works ($\delta D_{CI} = +98‰ \pm 99‰$, $\delta D_{CV} = -46‰ \pm 62‰$, $\delta D_{Paris} = -69‰ \pm 163‰$; Piani et al. 2021, Figure 3). These values are also consistent with the D/H measured in Orgueil by SIMS using an oxygen primary beam ($\delta D_{Orgueil} = -63‰ \pm 31‰$; Van Kooten et al. 2018). This method favors the hydrogen emission from the silicate relative to organics and is considered as a direct measurement of their C-free hydrous silicate D/H ratios (Deloule & Robert 1995). These values are significantly higher than (i) the D/H measured for hydrous minerals in the CM carbonaceous chondrite Mighei determined

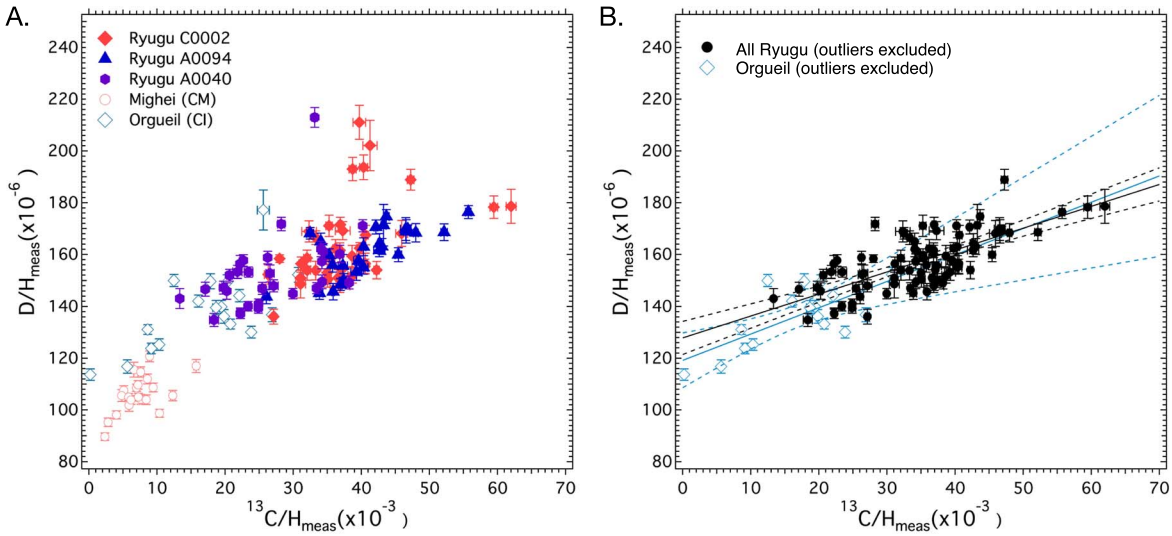

Figure 2. Measured D^-/H^- vs. $^{13}C^-/H^-$ ratios in Ryugu's particles, the Murchison (CM), and the Orgueil (CI) carbonaceous chondrites (raw data). All data were acquired in the same analytical session in 2022 March. Linear fits (solid lines) and 95% confidence interval bands (dashed lines) are shown for all Ryugu's points and for Orgueil chondrite with the exception of points outside the prediction interval at 95% confidence (see Section 4.2 and Figure A4 for details). Error bars represent 2σ internal errors.

here (Table 1) and (ii) the average for CM chondrite hydrous minerals determined using bulk ($\delta D_{CM,bulk} = -444‰ \pm 46‰$, 2σ; Alexander et al. 2012) or (iii) previous in situ measurements ($\delta D_{CM,\ in\ situ} = -350‰ \pm 40‰$, 2σ; Piani et al. 2018; Van Kooten et al. 2018; Figure 3) with the exception of the least altered lithologies of the CM chondrite Paris. It is also significantly lower than the hydrous mineral D/H ratio of the ungrouped carbonaceous chondrites Bells and Essebi ($\delta D_{Bells/Essebi} = +380‰ \pm 64‰$; Piani et al. 2021; Figure 3). Given the presence of a well-defined correlation between the C/H and D/H ratios measured in Ryugu ($R_{Pearson} = 0.72$; Table 1), the consistency with D/H ratios of hydrous minerals in Orgueil and Alais CI chondrites using the same method (Table 1 and Piani et al. 2021) and in Orgueil using a SIMS oxygen primary beam (Van Kooten et al. 2018), the possibility of a significant contribution of another hydrogen-bearing component such as NH_3 appears unlikely. Indeed, this third component would have to be so well mixed within chondritic material that it gives a rather constant contribution at a 10 μm scale, regardless of whether a Ryugu particle or CI chondrite fragment is considered and regardless of the relative proportion of hydrous minerals and organic compounds of the analyzed area. It is also unlikely that this third component contributes similarly to the D/H estimates of hydrous minerals that were measured with two different SIMS configurations (oxygen versus cesium primary ions). Because the main hydrogen-bearing inorganic phases in Ryugu's rocks and in carbonaceous chondrite matrices correspond to hydrous silicates (serpentine and saponite) and because the equilibrium isotopic fractionation factor between hydrated silicates and water is smaller than the D/H reproducibility on the reference materials, we consider the zero intercept to be a direct proxy for the D/H ratio of the water from which the minerals formed (Piani & Marrocchi 2018).

The data obtained for Ryugu's particles follow the same trend as the data obtained for Orgueil in the same SIMS session but generally have higher C/H and D/H ratios (Figure 2). This is in agreement with bulk measurements showing that Ryugu's rocks contain less hydrogen and higher C/H ratios than CIs (Yokoyama et al. 2023). At first glance, the resemblances between the Ryugu, CI, and terrestrial ocean D/H ratios (Figure 3) prevent us from distinguishing between the hypotheses of (1) a higher loss of water to space from Ryugu's parent asteroid compared to CI chondrites or (2) the addition to CI chondrites of a few tens of percent of terrestrial hydrogen contamination. However, the similarity observed between CI and Ryugu water D/H despite different storage conditions and the fact that phyllosilicate-rich CM chondrites show D-poor water compared to terrestrial water by using the same in situ method demonstrate that our technique is only marginally affected by terrestrial contamination. Conversely, the bulk water concentration of Orgueil could be strongly affected by terrestrial contamination and recent pre-degassed measurements reevaluated a water abundance of around 8.5 wt.% (Vacher et al. 2020), not too far from the 6.84 wt.% determined for Ryugu's samples (Yokoyama et al. 2023). Altogether, this suggests that (i) Ryugu's parent body experienced limited water loss to space, in good agreement with the low temperature experienced after aqueous alteration (i.e., <100°C; Yokoyama et al. 2023) and (ii) in situ D/H estimate of the very fresh samples returned from Ryugu is certainly our best proxy for the water D/H signature of the CI-like material.

4.2. Nature of the D-rich Outliers

Five among the 95 analyses obtained for Ryugu's particles and one among the 18 analyses obtained for Orgueil show a significant enrichment in D/H accompanied by a medium C/H ratio (Figures 2(A); A4). These points, hereafter referred to as D-rich outliers, were also occasionally observed in previous measurements of unmetamorphosed carbonaceous chondrites (Piani et al. 2018, 2021). The relatively moderate C/H ratios of these D-rich outliers (Figures 2(A); A4) and the limited D-enrichments found for the IOM isolated from Ryugu's rocks compared to CI or CM chondrites ($\delta D \sim +400‰$ obtained from bulk mass spectrometry in Yabuta et al. 2023; $\delta D \sim +530‰$ obtained by NanoSIMS in Ito et al. 2022) preclude them from simply being interpreted as IOM-rich areas. The

[53] doi:10.24396/ORDAR-107

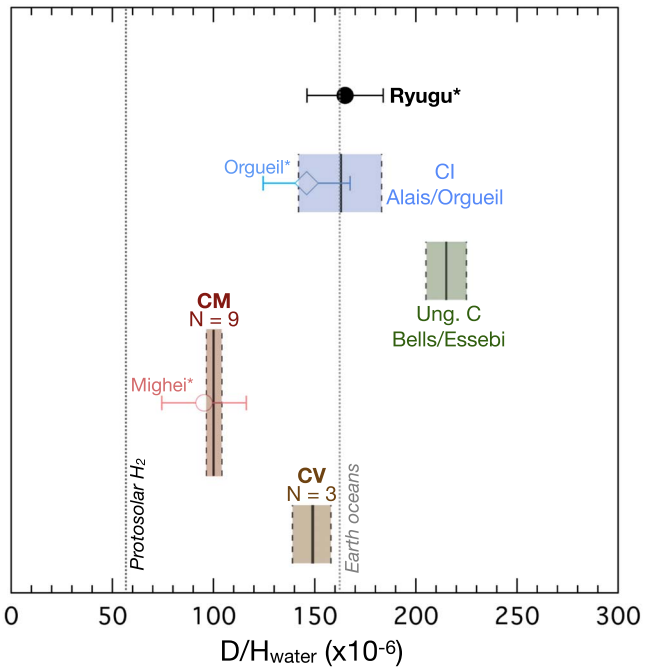

Figure 3. Hydrogen isotopic values (δD) estimated for water from the D/H vs. C/H correlation measured by SIMS for Ryugu, Orgueil, and Mighei (this study, indicated by a star) and compared to the range estimated previously for the different carbonaceous chondrite groups (Piani et al. 2021). Error bars indicate the 95% error estimated from SIMS analyses of the samples and standards for Ryugu, Orgueil, and Mighei. Solid lines and dashed lines indicate averages and two standard errors on the measurements for each chondrite group. For reference, the D/H ratios of the protosolar H_2 and the Earth oceans are also reported in the figure (Geiss & Gloecker 2003).

D-rich outliers could rather correspond to areas including one or several submicron-sized D-rich organic hot spots as observed by ion imaging both in Ryugu's bulk particles (either IOM or soluble organics) and in IOM (δD up to +8000‰; Yabuta et al. 2023) and more generally in pristine carbonaceous chondrites (e.g., Remusat et al. 2010). Interestingly, the highest D-enrichments were reported in the intact Ryugu grains instead of the isolated IOM (Yabuta et al. 2023) and could thus correspond to soluble organic compounds. Ito et al. (2022) also observed a generally higher D/H ratio (δD up to +840‰) for aliphatic-rich organics than in the entire C-rich region (δD up to +530‰), confirming the possible D-richest nature of some (possibly soluble) organic compounds. Further D/H and C/H investigations using high-resolution ion imaging by NanoSIMS would help better constrain the nature of the D-rich outliers observed in the present study.

4.3. Implications for the Origin and Distribution of Water in the Protoplanetary Disk and on Earth

Our results confirm the similarity of Ryugu samples to the CI carbonaceous chondrites (Figure 3), a conclusion already reached based on several other chemical and isotopic signatures (e.g., Ito et al. 2022; Nakamura et al. 2022a, 2022b; Yokoyama et al. 2023). The primitiveness of the Ryugu's material allows the signature of its water and whole rock hydrogen to be considered a reference value when discussing the distribution of hydrogen in the planetary materials of the early solar system. In particular, the resemblance between the D/H of Ryugu's water and the terrestrial oceans (Figure 3) and the slight D-enrichment of the bulk samples compared to CI chondrites can be used to reevaluate the role of CI-like material as a possible contributor to the water on Earth and the other rocky planets (Alexander et al. 2012; Marty 2012; Peslier et al. 2017; McCubbin & Barnes 2019; Piani et al. 2020). Enstatite chondrites (EC) are commonly proposed to resemble the main Earth's building blocks due their similarity with terrestrial rocks for a number of different isotopic systems, including hydrogen (Javoy et al. 2010; Dauphas 2017; Piani et al. 2020). Nevertheless, terrestrial surficial reservoirs have D-rich isotopic composition relative to ECs and the Earth's mantle, which points toward an additional contribution of CI-like materials to the Earth's surficial reservoirs (Piani et al. 2020). Considering the bulk H-content (Yokoyama et al. 2023) and the bulk H-isotopic composition (Naraoka et al. 2023) of Ryugu's particles as representative of the uncontaminated signature of CI chondrites, we find a ~3 wt.% contribution from CI-like material to Earth's surficial reservoir that would account for about 30% of the total mass of water in the oceans. Indeed, the lower H abundance for Ryugu's bulk rock relative to CI chondrites compensates for its lower D/H ratio in the mass balance calculation. Such an estimate is consistent with those obtained from noble gases, molybdenum, and zinc isotopes (Marty 2012; Budde et al. 2019; Paquet et al. 2022; Savage et al. 2022; Steller et al. 2022) and thus supports the importance of Ryugu material for establishing the characteristics and conditions of habitability in our planet.

A surprising characteristic of the hydrogen isotopic composition of Ryugu/CI water is its moderate D-enrichment (Figure 3). Indeed, CI chondrites likely accreted in the outer solar system (Gounelle et al. 2006; Desch et al. 2018), where water ices are expected to have large D-excesses (Jacquet & Robert 2013; Kavelaars et al. 2011; Hopp et al. 2022) and as illustrated by the generally high D/H ratios measured in comets (Müller et al. 2022). Although secondary parent body processes could have modified the hydrogen isotopic compositions of chondritic waters (Alexander et al. 2010; Sutton et al. 2017), through aqueous oxidation of Fe-Ni metal beads followed by H_2 loss and Rayleigh-like isotopic fractionation, this process is not expected to produce large isotopic changes in water-rich meteorites such as CIs (Alexander et al. 2010). Alternatively, the water could have been enriched in D by hydrogen isotopic exchange with D-rich IOMs. This process, if it was more efficient for Ryugu than for other CI chondrites, could explain the lower D/H measured for Ryugu's IOM compared to CI IOMs (Yabuta et al. 2023) but would only marginally increase the water D/H (from about −100‰ to +59‰). It is difficult to draw conclusions with our data on the efficiency of such hydrogen isotopic exchanges, due to the large uncertainties of the D/H ratios (±120‰). It is also unclear why exchanges would have been more pronounced in Ryugu's parent body than in the CI parent body, as similar temperatures and durations were proposed for Ryugu and CI secondary alteration (Yokoyama et al. 2023). As disk ionization processes do not significantly enrich water in D (Cleeves et al. 2014; Laurent et al. 2015), our results rather suggest that the Ryugu/CI water was inherited from the molecular cloud but underwent isotopic re-equilibration with the D-poor H_2 gas of the circumsolar disk and/or mixing with water formed at higher temperature (Piani et al. 2021) or D-rich water destruction driven by ultraviolet photons in the outermost layers of ice-coated grains (Furuya et al. 2017) before accretion onto the CI parent body. Altogether, this confirms the importance of Ryugu samples

for understanding the processes that prevailed during the disk evolution and shaped the surficial characteristics of terrestrial planets.

5. Closing Remarks

Using in situ SIMS measurements, we estimated the hydrogen isotopic composition of hydrous minerals present in Ryugu's samples: $\delta D_{Ryugu} = +59‰ \pm 121‰$ (2σ). This estimate is in good agreement with previous data reported for CI chondrites. Considering the highly pristine nature of Ryugu's samples, these values represent our best estimate of water in CI-like material. Combined with literature studies, our data suggest that (i) Ryugu's parent body experienced limited water loss to space and (ii) Ryugu/CI water is derived from D-enriched interstellar water that underwent re-equilibration during the evolution of the disk. Based on our new isotopic estimate of CI water, we also reevaluated the mass contribution of CI-like material to the Earth's surficial reservoirs to be ~3%.

This work was carried out under the auspices of the Hayabusa2 Initial Analysis Team "Chemistry" led by Prof. H. Yurimoto. Nordine Bouden is warmly thanked for helpful technical assistance for SIMS sample preparation and SIMS measurements. Yves Marrocchi is warmly thanked for help for data acquisition and for meaningful discussions throughout the course of this project. We thank an anonymous reviewer for constructive reviews and comments. This work was supported by the Centre national d'études spatiales (CNES) and by l'Agence Nationale de la Recherche (ANR) through grant ANR-19-CE31-0027-01 HYDRaTE (PI Laurette Piani). This is CRPG contribution #2831.

Appendix
Data availability

Series of tables including SIMS data obtained on standards and samples (raw data corrected from dead time and linear drift) can be found at the OTELo Research Data Repository (ORDaR).[54]

A.1. Details of the SIMS Analytical Conditions

A Cs^+ primary beam accelerated to 10 kV was used for the measurements. The vacuum in the analytical chamber was always below 3×10^{-9} mbar. Prior to analyses, the samples were presputtered at high current (2.5 nA) for 4 minutes to clean the sample surface, remove the adsorbed H and gold coating, and reach the sputtering steady state. The samples were then sputtered with a 50–500 pA beam rastered over a 30×30 μm^2 area. A high-magnification mode (Max Area 40) and a small field aperture (FA 2000) were used to minimize H contamination that would diffuse from the borders of the beam. A normal-incidence electron gun was used for charge compensation. The analyzed area was additionally restricted to a 12×12 μm^2 area in the center of the rastered area by using a 40% electronic gate to remove H coming from the borders of the rastered area. H^-, D^-, $^{13}C^-$, and $^{29}Si^-$ ions were collected successively by changing the magnetic field and counted with the monocollection electron multiplier. The mass resolving power was set to $M/\Delta M = 3300$ to avoid interferences on $^{13}C^-$ by $^{12}CH^-$ and on $^{29}Si^-$ by $^{28}SiH^-$. For each analysis, 30 cycles were collected with 2 s of counting time per cycle for H^-, $^{13}C^-$, and $^{29}Si^-$ and 20 s per cycle for D^-, totaling 30 minutes per analysis. ^{13}C was measured instead of ^{12}C because its lower abundance allows for the measurement of carbon with the electron multiplier across the entire range of C concentrations in standards and samples.

Figure A1 and A2 provide BSE images and X-ray elemental maps acquired by energy dispersive spectroscopy of analysed areas in particule A0094 and C0002. Figure A3 presents the standard calibrations for SIMS D/H measurements. Figure A4 presents the measured D/H vs. $^{13}C/H$ ratios in the Ryugu's particles and the CI chondrite Orgueil with their confidence and prediction interval bands at 95% used to defined the outliers points discussed in Section 4.2.

Table A1
Reference Values and Averages of the SIMS Measurements

Name	Type	D/H_{ref} ($\times 10^{-6}$)	H_2O_{ref} (wt%)	References	N	D^-/H^- ($x10^{-6}$)	2SD ($x10^{-6}$)	2SE ($x10^{-6}$)	IMF	2SE
M98-47963	Basaltic glass	144	1.45	a	10	130	13.5	4.3	0.90	0.03
Tan25-0	Andesitic glass	127	0.85	b	11	97.4	5.6	1.7	0.77	0.01
Etna-4	Basaltic glass	135	3.64	b	16	115	7.8	2.0	0.85	0.01
Serp-12A	Serpentine	145	12.20	c	3	132	3.8	2.2	0.91	0.01
Mtm	Montmorillonite	143	4.61	d	10	123	13.8	4.4	0.86	0.03
Kipawa	Amphibole	142	1.50	e	17	119	13.2	3.2	0.84	0.02
Bamble	Amphibole	146	2.30	e	2	119	5.3	3.7	0.81	0.03
IOM GRO	IOM from GRO 95502	669	...	d	25	353	40.2	8.0	0.53	0.01
IOM Orgueil	IOM from Orgueil	307	...	f	13	193	28.1	7.8	0.63	0.03
KerIII	Type-III kerogen	141	...	d	15	101	10.8	2.8	0.72	0.02

Note. N = number of analyses; SD = standard deviation; SE = standard errors; IMF = instrumental mass fractionation.
References: (a) Bindeman et al. 2012, (b) Métrich & Deloule (2014), (c) Selverstone & Sharp 2013, (d) Piani et al. 2012, (e) Deloule & Robert 1995, (f) Remusat et al. 2009.

[54] doi:10.24396/ORDAR-107

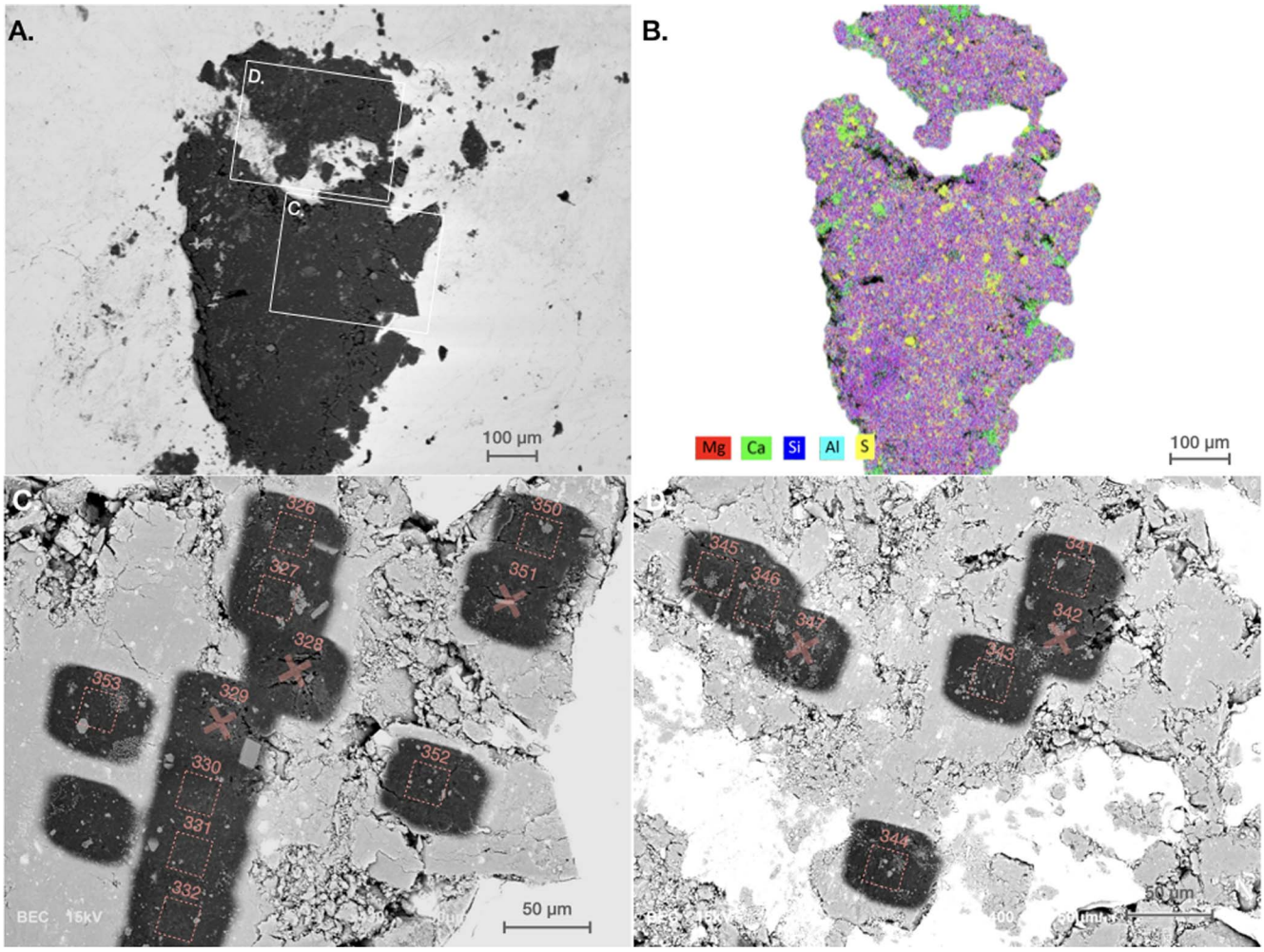

Figure A1. Scanning electron microscope (SEM) images of a piece of particle A0094 pressed in indium and location of the SIMS analyses. (A) Backscattered electron (BSE) image of the pressed particle fragment before SIMS analyses. (B) Combined X-ray elemental map of the particle fragment. The particle is dominated by Mg-rich phyllosilicates (purple), sulfides (yellow), and carbonates (light green). Large holes and cracks (black) were avoided for SIMS analyses. (C)–(D) BSE images of areas measured by SIMS. The numbers correspond to the analysis numbers as provided on ORDaR.[55] Red crosses indicate analyses that were rejected due to small holes or cracks identified by SEM after the SIMS measurements.

[55] doi:10.24396/ORDAR-107

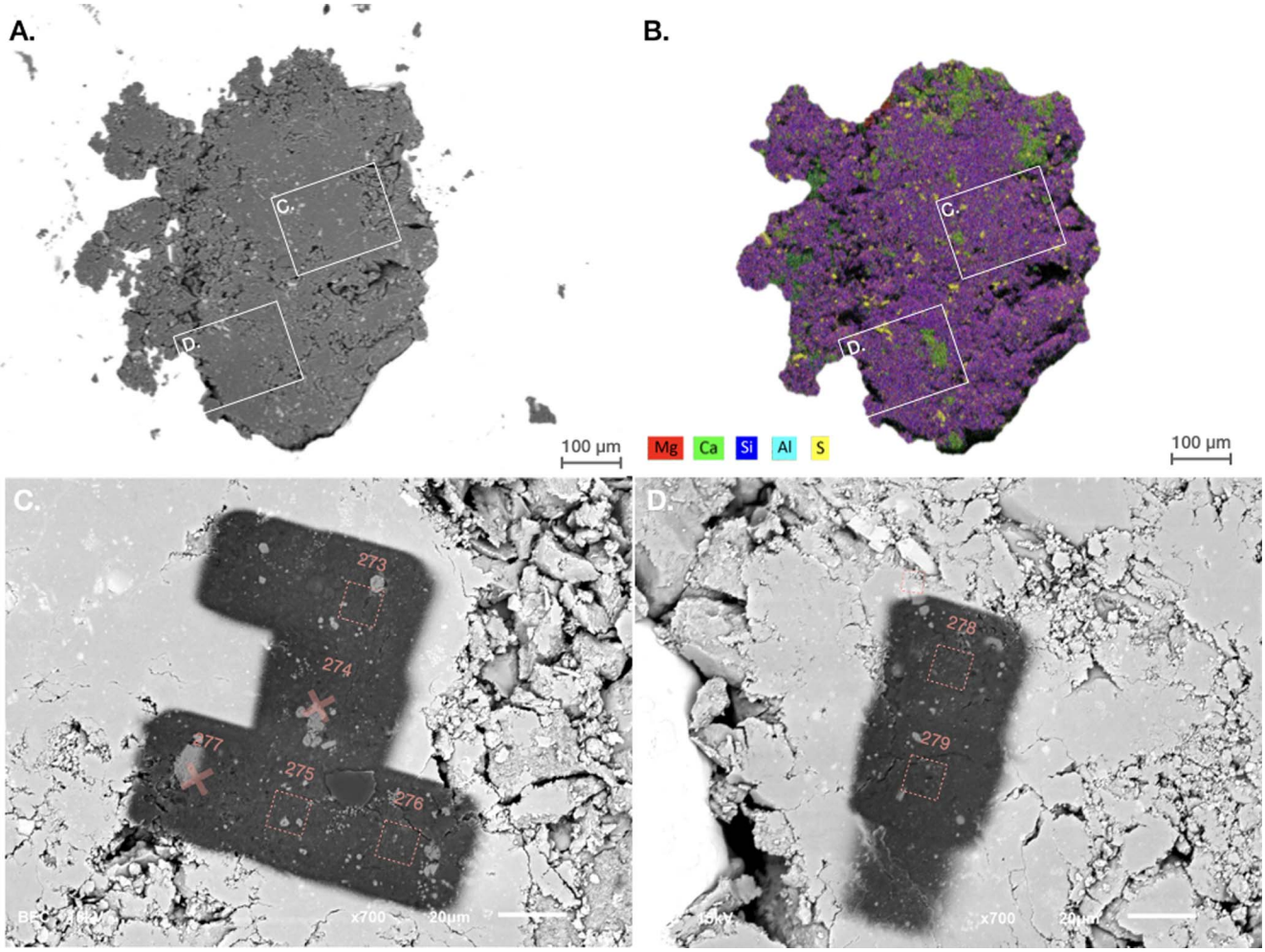

Figure A2. Scanning electron microscope (SEM) images of a piece of particle C0002 pressed in indium and location of the SIMS analyses. (A) Backscattered electron (BSE) image of the pressed particle fragment before SIMS analyses. (B) Combined X-ray elemental map of the particle fragment. The particle is dominated by Mg-rich phyllosilicates (purple), sulfides (yellow), and carbonates (light green). Large holes and cracks (black) were avoided for SIMS analyses. (C)–(D) BSE images of areas measured by SIMS. The numbers correspond to the analysis numbers as provided on ORDaR. [56] Red crosses indicate analyses that were rejected due to small holes or cracks identified by SEM after the SIMS measurements.

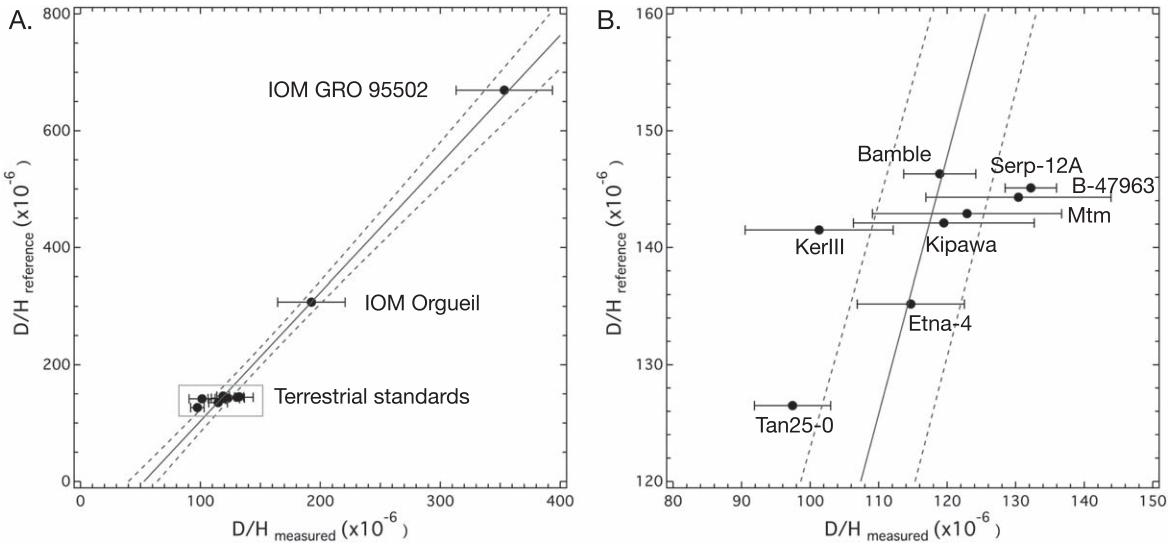

Figure A3. Calibration line of the D/H ratios. The calibration includes the different standards analyzed during the session (Table A1) and allows the correction of the instrumental mass fractionation and surface contamination following previous works (Remusat et al. 2016; Piani et al. 2018, 2021).

[56] doi:10.24396/ORDAR-107

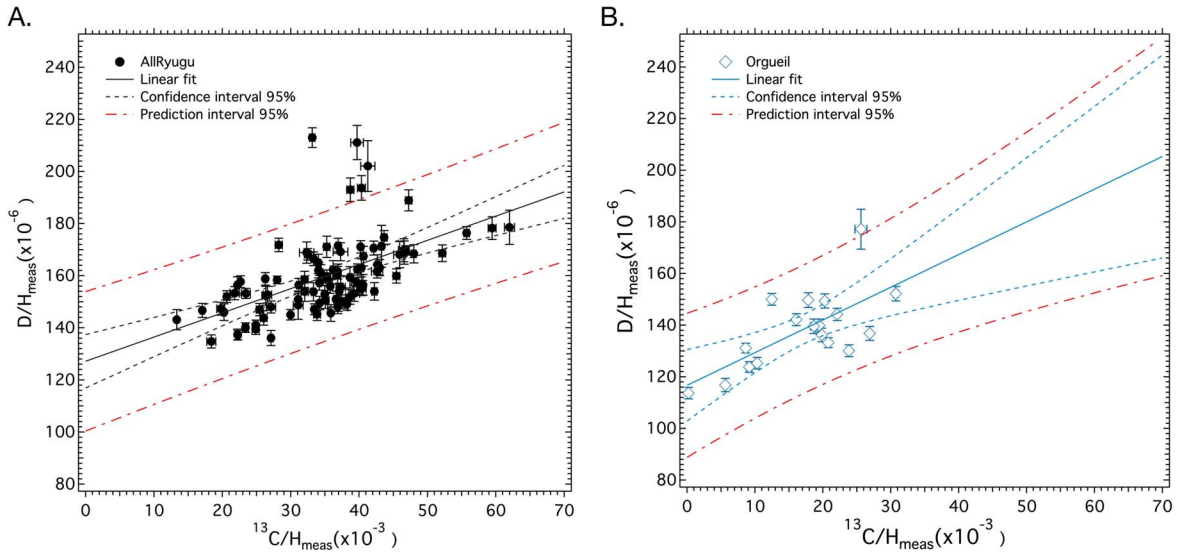

Figure A4. Measured D/H vs. $^{13}C/H$ ratios in (A) the Ryugu's particles and (B) the CI chondrite Orgueil with their confidence and prediction interval bands at 95%. All points lying outside of the prediction interval bands are considered outliers and are not included in the main trend estimate for the final estimation of the water D/H ratios (Table 1).

ORCID iDs

Laurette Piani https://orcid.org/0000-0003-0854-7468
Naoya Sakamoto https://orcid.org/0000-0003-2335-1359
Conel M. O'D. Alexander https://orcid.org/0000-0002-8558-1427
Sachiko Amari https://orcid.org/0000-0003-4899-0974
Martin Bizzarro https://orcid.org/0000-0001-9966-2124
Audrey Bouvier https://orcid.org/0000-0002-8303-3419
Richard W. Carlson https://orcid.org/0000-0001-7195-2074
Marc Chaussidon https://orcid.org/0000-0001-8475-0690
Andrew M. Davis https://orcid.org/0000-0001-7955-6236
Wataru Fujiya https://orcid.org/0000-0003-2578-5521
Ryota Fukai https://orcid.org/0000-0002-1477-829X
Ikshu Gautam https://orcid.org/0000-0002-0415-9428
Yuki Hibiya https://orcid.org/0000-0002-3346-9820
Hiroshi Hidaka https://orcid.org/0000-0001-7239-4086
Hisashi Homma https://orcid.org/0000-0002-3662-577X
Peter Hoppe https://orcid.org/0000-0003-3681-050X
Gary R. Huss https://orcid.org/0000-0003-4281-7839
Tsuyoshi Iizuka https://orcid.org/0000-0001-7896-5812
Akira Ishikawa https://orcid.org/0000-0002-8938-0200
Kouki Kitajima https://orcid.org/0000-0001-7634-4924
Yuki Masuda https://orcid.org/0000-0002-7704-0014
Mayu Morita https://orcid.org/0000-0001-5769-7687
Kazuko Motomura https://orcid.org/0000-0002-1635-7173
Ann Nguyen https://orcid.org/0000-0002-0442-1991
Changkun Park https://orcid.org/0000-0002-1206-6803
Maria Schönbächler https://orcid.org/0000-0003-4304-214X
Lauren Tafla https://orcid.org/0000-0003-4565-2654
Haolan Tang https://orcid.org/0000-0002-9293-3662
Sohei Wada https://orcid.org/0000-0001-6723-0378
Meenakshi Wadhwa https://orcid.org/0000-0001-9187-1255
Richard J. Walker https://orcid.org/0000-0003-0348-2407
Qing-Zhu Yin https://orcid.org/0000-0002-4445-5096
Tetsuya Yokoyama https://orcid.org/0000-0003-2247-7232
Shigekazu Yoneda https://orcid.org/0000-0003-2306-4261
Edward D. Young https://orcid.org/0000-0002-1299-0801
Ai-Cheng Zhang https://orcid.org/0000-0002-5758-0726
Hiroshi Naraoka https://orcid.org/0000-0002-2373-8759
Ryuji Okazaki https://orcid.org/0000-0003-0177-7527
Tatsuaki Okada https://orcid.org/0000-0001-6381-8107
Toru Yada https://orcid.org/0000-0002-7971-510X
Satoru Nakazawa https://orcid.org/0000-0003-4250-1826
Satoshi Tanaka https://orcid.org/0000-0002-4874-0417
Sei-ichiro Watanabe https://orcid.org/0000-0002-5820-2102
Makoto Yoshikawa https://orcid.org/0000-0002-3118-7475
Shogo Tachibana https://orcid.org/0000-0002-4603-9440
Hisayoshi Yurimoto https://orcid.org/0000-0003-0702-0533

References

Alexander, C. M. O'D., Bowden, R., Fogel, M. L., & Howard, K. T. 2015, M&PS, 50, 810
Alexander, C. M. O'D., Bowden, R., Fogel, M. L., et al. 2012, Sci, 337, 721
Alexander, C. M. O'D., Fogel, M., Yabuta, H., & Cody, G. D. 2007, GeCoA, 71, 4380
Alexander, C. M. O'D., Newsome, S. D., Fogel, M. L., et al. 2010, GeCoA, 74, 4417
Bindeman, I. N., Kamenetsky, V. S., Palandri, J., & Vennemann, T. 2012, ChGeo, 310, 126
Budde, G., Burkhardt, C., & Kleine, T. 2019, NatAs, 3, 736
Cleeves, L. I., Bergin, E. A., Alexander, C. M. O'D., et al. 2014, Sci, 345, 1590
Dauphas, N. 2017, Natur, 541, 521
Deloule, E., & Robert, F. 1995, GeCoA, 59, 4695
Desch, S. J., Kalyaan, A., & Alexander, C. M. O. 2018, ApJS, 238, 11
Furuya, K., Drozdovskaya, M. N., Visser, R., et al. 2017, A&A, 599, A40
Geiss, J., & Gloecker, G. 2003, SSRv, 106, 3
Gounelle, M., Spurný, P., & Bland, P. A. 2006, M&PS, 41, 135
Hopp, T., Dauphas, N., Abe, Y., et al. 2022, SciA, 8, 8141
Ito, M., Tomioka, N., Uesugi, M., et al. 2022, NatAs, 6, 1163
Jacquet, E., & Robert, F. 2013, Icar, 223, 722
Javoy, M., Kaminski, E., Guyot, F., et al. 2010, E&PSL, 293, 259
Kavelaars, J. J., Mousis, O., Petit, J. M., & Weaver, H. A. 2011, ApJL, 734, L30
Laurent, B., Roskosz, M., Remusat, L., et al. 2015, NatCo, 6, 8567
Marty, B. 2012, E&PSL, 313, 56
McCubbin, F. M., & Barnes, J. J. 2019, E&PSL, 526, 115771

Métrich, N., & Deloule, E. 2014, Litho, 206, 400
Moynier, F., Dai, W., Yokoyama, T., et al. 2022, GChPL, 24, 1
Müller, D. R., Altwegg, K., Berthelier, J. J., et al. 2022, A&A, 662, A69
Nakamura, E., Kobayashi, K., Tanaka, R., et al. 2022b, PJAB, 98, 227
Nakamura, T., Matsumoto, M., Amano, K., et al. 2022a, Sci, 8671, 2003
Naraoka, H., Takano, Y., Dworkin, J. P., et al. 2023, Sci, 379, 9033
Paquet, M., Moynier, F., Yokoyama, T., et al. 2023, NatAs, 7, 182
Peslier, A. H., Schönbächler, M., Busemann, H., & Karato, S. I. 2017, SSRv, 212, 1
Piani, L., & Marrocchi, Y. 2018, E&PSL, 504, 64
Piani, L., Marrocchi, Y., Rigaudier, T., et al. 2020, Sci, 369, 1110
Piani, L., Marrocchi, Y., Vacher, L. G., Yurimoto, H., & Bizzarro, M. 2021, E&PSL, 567, 117008
Piani, L., Remusat, L., & Robert, F. 2012, AnaCh, 84, 10199
Piani, L., Yurimoto, H., & Remusat, L. 2018, NatAs, 2, 317
Remusat, L., Guan, Y., Wang, Y., & Eiler, J. M. 2010, ApJ, 713, 1048
Remusat, L., Piani, L., & Bernard, S. 2016, E&PSL, 435, 36
Remusat, L., Robert, F., Meibom, A., et al. 2009, ApJ, 698, 2087
Robert, F., & Epstein, S. 1982, GeCoA, 46, 81
Savage, P. S., Moynier, F., & Boyet, M. 2022, Icar, 386, 115172
Selverstone, J., & Sharp, Z. D. 2013, GGG, 14, 4370
Steller, T., Burkhardt, C., Yang, C., & Kleine, T. 2022, Icar, 386, 115171
Sutton, S., Alexander, C. M. O'D., Bryant, A., et al. 2017, GeCoA, 211, 115
Tachibana, S., Sawada, H., Okazaki, R., et al. 2022, Sci, 375, 1011
Vacher, L. G., Piani, L., Rigaudier, T., et al. 2020, GeCoA, 281, 53
Van Kooten, E. M. M. E., Cavalcante, L. L., Nagashima, K., et al. 2018, GeCoA, 237, 79
Viennet, J. C., Le Guillou, C., Remusat, L., et al. 2022, GeCoA, 318, 352
Yabuta, H., Cody, G. D., Engrand, C., et al. 2023, Sci, 379, 9057
Yamashita, Y., & Naraoka, H. 2014, GeocJ, 48, 519
Yokoyama, T., Nagashima, K., Nakai, I., et al. 2023, Sci, 379, 7850